

C–N Activation versus Metalation: Reaction of Bis(methylzinc) 1,2-Bis((*tert*-butyldimethylsilyl)amido)-1,2-dipyridylethane with Acetamide and Aniline

Matthias Westerhausen,* Tobias Bollwein, Konstantin Karaghiosoff, Stefan Schneiderbauer,† Martin Vogt,† and Heinrich Nöth†

Department Chemie, Ludwig-Maximilians-Universität München, Butenandtstrasse 9 (House D), D-81377 Munich, Germany

Received October 3, 2001

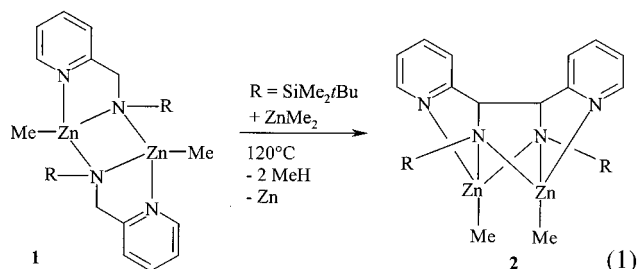
The protonation of racemic (1*S*,2*S*)-bis(methylzinc) and (1*R*,2*R*)-bis(methylzinc) 1,2-bis((trialkylsilyl)amido)-1,2-dipyridylethane (**2**) with acetamide quantitatively yields racemic 1,2-bis((trialkylsilyl)amino)-1,2-dipyridylethane (**3**); the meso form **4** is not observed. Irradiation of **3** leads to an equilibrium mixture of all possible isomers, which have been detected by NMR spectroscopy. The crystal structures of **3** and **4** show elongated C–C bonds of the ethane backbone. Recrystallization of **3** from a water/acetone mixture resulted in precipitation of a water adduct of **3**, which crystallizes in a chain structure with weak hydrogen bridges. The reaction of **2** with aniline gave bis(methylzinc) 1,2-bis(phenylamido)-1,2-dipyridylethane (**5**). Experiments with ¹⁵N-labeled aniline show that, however, the C–N, not the Si–N, bonds are cleaved.

Introduction

Organozinc compounds are widely used reagents in organic and organometallic chemistry, due to their rather low reactivity and their intolerance toward a wide variety of functional groups.^{1,2} In some cases the use of catalysts which contain d-block metals is necessary to raise the reactivity.³ In general, the increasing ionicity of the metal–carbon bonds enhances their reactivity. Therefore, the Zn–C bonds are less reactive than the Mg–C bonds in isostructural compounds. Two factors offer the possibility of enhancing the reactivity of organozinc compounds. The coordination of aromatic nitrogen compounds such as pyridine and bipyridine^{4,5} leads to an unusually high reactivity. One notable example is the synthesis and isolation of a bis-zincated methane, which was effected by using pyridyl anchors at antimony compounds to enable an antimony–zinc exchange reaction.⁶ Another example for such high reactivity is the activation of carbon dioxide by zinc complexes⁷ such as the tris(pyrazolato)borane complex as a model for the carboxylase.⁸ The reactivity also can

be enhanced by having two metal centers in very close contact to each other,⁹ as shown in a variety of biologically relevant compounds such as peptidases and phosphatases.^{10–12}

A tetradentate ligand which is able to bind two metal centers in very close contact to each other is easily accessible. The metalation of (trialkylsilyl)(2-pyridylmethyl)amine with dimethylzinc gave quantitatively dimeric methylzinc (trialkylsilyl)(2-pyridylmethyl)amide (**1**). Heating this compound in the presence of dimethylzinc for several hours resulted in precipitation of zinc metal and C–C bond formation according to eq 1.



Cooling the solution yielded bis(methylzinc) 1,2-bis((trialkylsilyl)amido)-1,2-dipyridylethane (**2**), which crystallized as a racemate of the *R,R* and *S,S* isomers.⁴

† Crystal structure determinations.

(1) Knochel, P.; Jones, P. *Organozinc Reagents-A Practical Approach*; University Press: Oxford, U.K., 1999.

(2) Frantz, D. E.; Fässler, R.; Tomooka, C. S.; Carreira, E. M. *Acc. Chem. Res.* **2001**, *33*, 373.

(3) Pu, L.; Yu, H.-B. *Chem. Rev.* **2001**, *101*, 757.

(4) (a) Westerhausen, M.; Bollwein, T.; Makropoulos, N.; Rotter, T. M.; Habeder, T.; Suter, M.; Nöth, H. *Eur. J. Inorg. Chem.* **2001**, 851. (b) Westerhausen, M.; Bollwein, T.; Makropoulos, N.; Schneiderbauer, S.; Suter, M.; Nöth, N.; Mayer, P.; Piotrowski, H.; Polborn, K.; Pfitzner, A. *Eur. J. Inorg. Chem.* **2002**, 389.

(5) Van Koten, G.; Jastrzebski, J. T. B. H.; Vrieze, K. *J. Organomet. Chem.* **1983**, *250*, 49.

(6) Andrews, P. C.; Raston, C. L.; Skelton, B. W.; White, A. H. *Organometallics* **1998**, *17*, 779.

(7) Kunert, M.; Bräuer, M.; Klobes, O.; Görls, H.; Dinjus, E.; Anders, E. *Eur. J. Inorg. Chem.* **2000**, 1803 and literature cited therein.

(8) Kimura, E. *Prog. Inorg. Chem.* **1994**, *41*, 443. Recent examples: (a) Looney, A.; Parkin, G.; Alsfasser, R.; Ruf, M.; Vahrenkamp, H. *Angew. Chem.* **1992**, *104*, 57; *Angew. Chem., Int. Ed. Engl.* **1992**, *31*, 92. (b) Ruf, M.; Schell, F. A.; Walz, R.; Vahrenkamp, H. *Chem. Ber./Recl.* **1997**, *130*, 101. (c) Rombach, M.; Maurer, C.; Weis, K.; Keller, E.; Vahrenkamp, H. *Chem. Eur. J.* **1999**, *5*, 1013.

(9) Marek, I. *Chem. Rev.* **2000**, *100*, 2887.

(10) Wilcox, E. *Chem. Rev.* **1996**, *96*, 2435.

(11) Sträter, N.; Lipscomb, W. N.; Klabunde, T.; Krebs, B. *Angew. Chem.* **1996**, *108*, 2158; *Angew. Chem., Int. Ed. Engl.* **1996**, *35*, 2024.

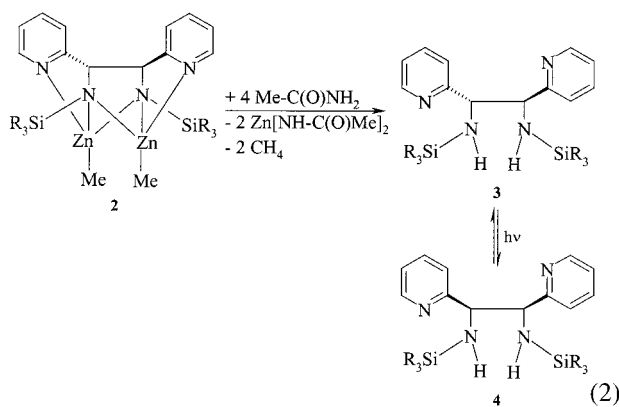
(12) Twitchett, M. B.; Sykes, A. G. *Eur. J. Inorg. Chem.* **1999**, 2105.

The central feature of bis(methylzinc) 1,2-bis((trialkylsilyl)amido)-1,2-dipyridylethane is the very close nonbonding contact of the zinc atoms of 2.72 Å, which is responsible for the unexpected reactivity of **2**. In contrast, complex **1** shows a Zn...Zn contact of 2.88 Å.⁴ The metalating properties of **2** toward (trialkylsilyl)-phosphines ($pK_a \approx 28$) or -arsines¹³ were demonstrated previously, whereas primary alkylamines ($pK_a \approx 35$) do not react with **2**. Therefore, we were interested in the reactions of complex **2** with acetamide ($pK_a \approx 25$) as well as aniline ($pK_a \approx 31$).

Discussion and Results

Synthesis. Hydrolysis is not a feasible route to obtain the protonated and metal-free ligand, namely 1,2-bis((trialkylsilyl)amino)-1,2-dipyridylethane (**3**), because the N–Si bonds are also attacked by water. Alcoholysis also is not practical for the same reason. There is a question regarding 1,2-bis((trialkylsilyl)amino)-1,2-dipyridylethane and its isomerization during the protonation reaction. Van Koten and co-workers observed equilibria between the monomeric radicals which formed due to a C–C bond cleavage and the dimers in the case of the N-alkylated derivative of the zinc complex **2**.¹⁴

Instead of water or alcohol and in accordance with eq 2, an excess of acetamide proved to be an adequate reagent to prepare quantitatively amine **3** without attack at the nitrogen–silicon functionalities. During

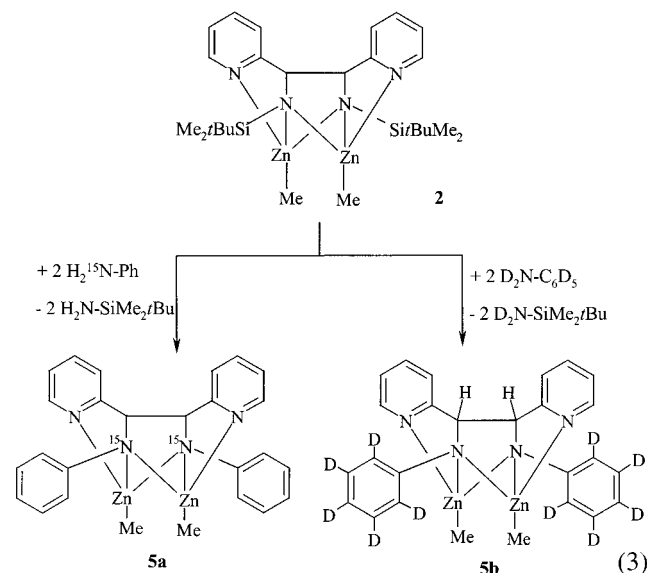


this reaction formation of the meso isomer was not observed. After methane evolution and precipitation of zinc bis(acetamide) the racemate of the *R,R* and *S,S* isomers of 1,2-bis((trialkylsilyl)amino)-1,2-dipyridylethane (**3**) was recrystallized from aliphatic hydrocarbons.

Compound **3** is air stable and nearly unreactive toward water. The recrystallization of **3** from a water/acetone mixture afforded a water adduct of **3** with a higher melting point than that of **3** itself. Isomerization of **3** did not occur in refluxing toluene, even after addition of small amounts of Lewis bases or acids such as metal halides and sodium hydroxide. Irradiation of

a hexane solution of **3** with a mercury lamp gave a mixture of all possible isomers, in which, after several days, the ratio of the racemate **3** to the meso form **4** approached approximately unity as determined by NMR spectroscopy (eq 2). In addition, (2-pyridylmethyl)(*tert*-butyldimethylsilyl)amine was formed. For comparison purposes the molecular structures of **3**, **3**·H₂O, and **4** were determined by X-ray diffraction. Without irradiation, solutions of **2**–**4** are EPR silent and there is no indication of an equilibrium with free radicals.

Whereas phosphines are metalated by the methylzinc group of compound **2**, aniline reacted in an unexpected manner. At first sight, the trialkylsilyl group was substituted by the phenyl group. To investigate whether it was the N–Si or a N–C bond that had been cleaved, [¹⁵N]aniline was used in this experiment. The NMR data clearly proved that the labeled nitrogen atoms were incorporated into the newly formed complex bis(methylzinc) 1,2-bis(phenyl[¹⁵N]amido)-1,2-dipyridylethane (**5a**). During this reaction the zinc-bonded methyl substituents did not show any metalating behavior. A reaction equation is given in eq 3. The dipyridyl molecule can



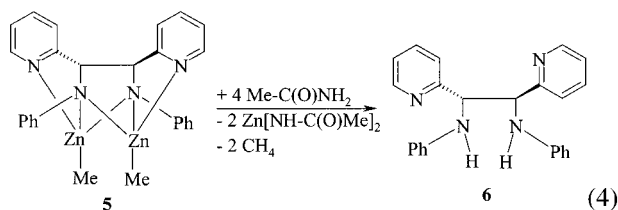
act as a hemilabile ligand¹⁵ in competition with the aniline molecule. After protonation of the silylated amido group, an anilide is formed, which attacks as a nucleophile the neighboring carbon atom. The next reaction step is proton migration. This leads to the formation of (trialkylsilyl)amine, which is eliminated.

To confirm this mechanism, deuterated aniline was used as a synthon in this reaction and the partly deuterated complex **5b** was isolated. The fact that after the substitution the protons of the ethane backbone were not replaced by deuterium atoms indicates that an elimination–addition mechanism can be excluded. The protolysis of **5** with acetamide gave 1,2-bis(phenylamino)-1,2-dipyridylethane (**6**; eq 4) in good yield as extremely thin needles not suitable for an X-ray structure determination. The quantitative separation from zinc bis(acetamide) failed due to similar solubility properties.

(13) Westerhausen, M.; Bollwein, T.; Warchhold, M.; Nöth, H. Z. Anorg. Allg. Chem. **2001**, 627, 1141.

(14) (a) Jastrzebski, J. T. B. H.; Klerks, J. M.; van Koten, G.; Vrieze, K. J. Organomet. Chem. **1981**, 210, C49. (b) Spek, A. L.; Jastrzebski, J. T. B. H.; van Koten, G. Acta Crystallogr. **1987**, C43, 2006. (c) Wissing, E.; van der Linden, S.; Rijnberg, E.; Boersma, J.; Smeets, W. J. J.; Spek, A. L.; van Koten, G. Organometallics **1994**, 13, 2602.

(15) Braunstein, P.; Naud, F. Angew. Chem. **2001**, 113, 702; Angew. Chem., Int. Ed. **2001**, 40, 680.



In contrast to these reactions, neither metalation nor incorporation of *tert*-butylamine was observed. Even in refluxing toluene a reaction of **2** with *t*Bu-NH₂ did not occur. The diversity of the reactions toward amides and amines might be correlated with the *pK_a* values. The rather acidic acetamide leads to a protolysis reaction of the zinc complexes without cleavage of the N–Si bond, whereas *tert*-butylamine with a *pK_a* value of approximately 35 is not able to protonate the nitrogen atoms of the C–C coupled zinc compounds. Aniline did protonate, but an S_N2 reaction followed and the insoluble phenyl-substituted zinc complex **5** precipitated.

Molecular Structures. The molecular structure of **3** as well as its numbering scheme are shown in Figure 1. The intramolecular steric strain can be seen from the rather long C1–C2 bond (1.563(2) Å) and widened C1–N3–Si1 as well as C2–N4–Si2 angles (129.5(1) and 127.6(1)°, respectively). Figure 2 represents the molecular structure of the meso form **4** and its numbering scheme. This centrosymmetric molecule shows structural parameters similar to those of **3**. The C1–C1' bond length is rather large (1.555(4) Å), and the C1–N1–Si1 bond angle is 128.6(2)°. The recrystallization of **3** from an acetone/water mixture yielded the 1/1 complex **3**·H₂O with a melting point much higher than that observed for **3**. The molecular structure of this C₂-symmetric complex is shown in Figure 3. The quality of the crystal structure determination allowed the isotropic refinement of the OH and NH functionalities and, therefore, permits a discussion of the hydrogen bridges. The water molecule shows contacts to the neighboring amino N atoms, thus leading to the tetra-coordinate oxygen atom O91 of the water molecule. The highly unsymmetrical hydrogen positions between the Lewis base sites (N1–H_{N1} and O91···H_{N1} = 0.75 and 2.28 Å and O91–H_{O91} and N63···H_{O91} = 0.91 and 2.00 Å, respectively) and the large O···N distances (O91···N1 = 3.01 Å and O91···N63 = 2.90 Å) are a sign of the presence of only weak hydrogen bridges. Nevertheless, these hydrogen contacts lead to the formation of a chain structure as represented in Figure 4, and thus, the higher melting point of **3** is explained. This chain is oriented along the crystallographic C₂ axis.

NMR Spectroscopy. Selected NMR parameters of the compounds **3**, **3**·H₂O, and **4** are summarized in Table 1. The numbering scheme for the assignment of these data is given in Figure 5. The stereocenters affect mainly the chemical shifts of the corresponding CH groups as well as the δ values of the chemically different silicon-bonded methyl substituents. The influence of the stereocenters on the *tert*-butyl groups is much smaller. The pyridyl ligands are hardly affected by the stereocenters or by the water molecule. The chemical shifts of the NH protons are also not influenced by the stereocenters or the water molecule, which accounts for the breakup of the chain structure in solution.

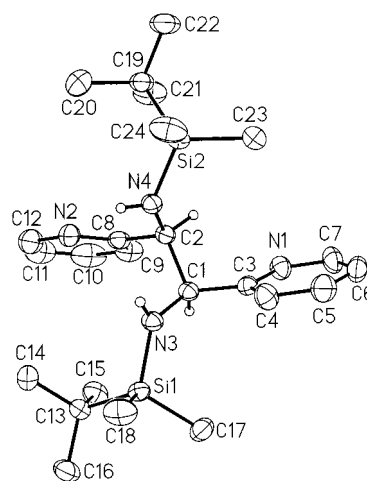


Figure 1. Molecular structure of (1*S*,2*S*)-1,2-dipyridyl-1,2-bis((*tert*-butyl)dimethylsilyl)aminoethane (**3**). The ellipsoids represent a 40% probability, whereas the hydrogen atoms bonding to C1, C2, N3, and N4 are drawn with arbitrary radii. All other hydrogen atoms are omitted for clarity. Selected bond lengths (Å): C1–C2 = 1.563(2), C1–C3 = 1.520(3), C2–C8 = 151.4(3), C1–N3 = 1.447(2), C2–N4 = 1.458(2), N3–Si1 = 1.716(2), N4–Si2 = 1.724(2), C3–C4 = 1.380(2), C4–C5 = 1.378(3), C5–C6 = 1.373(3), C6–C7 = 1.374(3), C7–N1 = 1.338(3), N1–C3 = 1.344(2), C8–C9 = 1.393(3), C9–C10 = 1.387(3), C10–C11 = 1.374(4), C11–C12 = 1.367(4), C12–N2 = 1.334(3), N2–C8 = 1.337(3). Selected bond angles (deg): C2–C1–C3 = 108.9(1), C2–C1–N3 = 110.4(1), C3–C1–N3 = 114.5(1), C1–N3–Si1 = 129.5(1), C1–C2–C8 = 109.9(1), C1–C2–N4 = 110.5(1), C8–C2–N4 = 113.0(1), C2–N4–Si2 = 127.6(1).

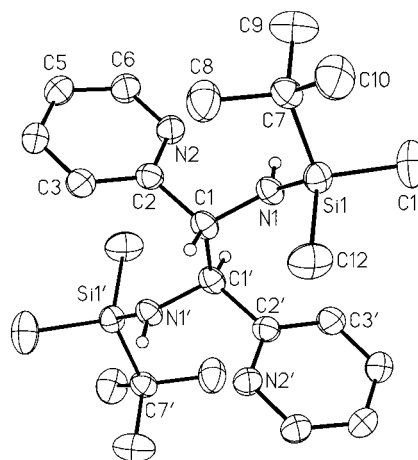


Figure 2. Molecular structure of (1*S*,2*R*)-1,2-dipyridyl-1,2-bis((*tert*-butyl)dimethylsilyl)aminoethane (**4**). The ellipsoids represent a 40% probability, whereas the hydrogen atoms bonding to C1 and N1 are drawn with arbitrary radii. All other hydrogen atoms are omitted for clarity. Symmetry-related atoms ($-x + 1, -y + 1, -z + 2$) are marked with primes. Selected bond lengths (Å): C1–C1' = 1.555(4), C1–C2 = 1.518(3), C1–N1 = 1.459(2), N1–Si1 = 1.712(2), C2–C3 = 1.392(3), C3–C4 = 1.373(3), C4–C5 = 1.371(4), C5–C6 = 1.377(3), C6–N2 = 1.340(3), N2–C2 = 1.338(3). Selected bond angles (deg): C1'–C1–C2 = 109.2(2), C1'–C1–N1 = 111.0(2), C2–C1–N1 = 112.1(2), C1–N1–Si1 = 128.6(2).

Table 2 contains the NMR data of the [¹⁵N]-labeled dinuclear zinc complex **5**. The numbering scheme is given in Figure 5. The signals due to the CH moieties of the central ethane backbone as well as the zinc-

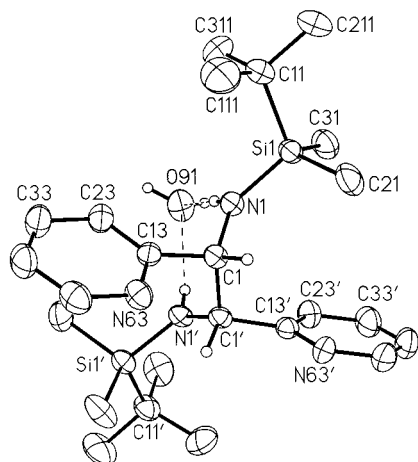


Figure 3. Molecular structure of the 1/1 water adduct of (1*R*,2*R*)-1,2-dipyridyl-1,2-bis((*tert*-butyldimethylsilyl)-amino)ethane (**3**·H₂O). The ellipsoids represent a 40% probability, whereas the hydrogen atoms bonding to C1, N1, and O91 are drawn with arbitrary radii. All other hydrogen atoms are omitted for clarity. Symmetry-related atoms are marked with primes. Selected bond lengths (Å): C1–C1' = 1.560(7), C1–C13 = 1.530(5), C1–N1 = 1.441(5), N1–Si1 = 1.710(4), C13–C23 = 1.371(6), C23–C33 = 1.390(6), C33–C43 = 1.363(6), C43–C53 = 1.365(6), C53–N63 = 1.336(5), N63–C13 = 1.346(5). Selected bond angles (deg): C1'–C1–C13 = 107.7(4), C1'–C1–N1 = 112.4(2), C13–C1–N1 = 115.2(3), C1–N1–Si1 = 129.4(3).

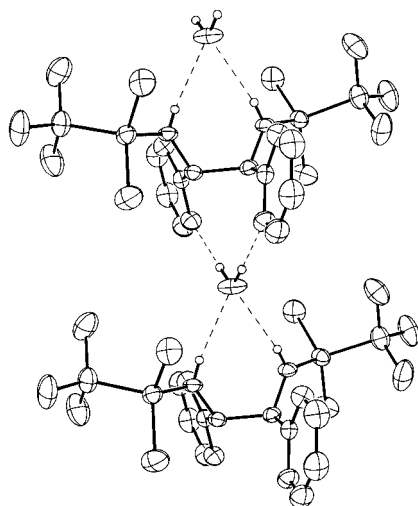


Figure 4. Chain structure of the 1/1 water adduct of (1*R*,2*R*)-1,2-dipyridyl-1,2-bis((*tert*-butyldimethylsilyl)-amino)ethane (**3**·H₂O) with the chains arranged parallel to the crystallographic *C*₂ axis. The ellipsoids represent a 40% probability, whereas the hydrogen atoms bonding to C1, N1, and O91 are drawn as circles. All other hydrogen atoms are omitted for clarity. Symmetry-related atoms are marked with primes. Hydrogen bridges are shown as dashed lines.

bonded methyl groups are only slightly shifted to lower field compared to those of the starting material **2**. In the ¹⁵N{¹H} NMR experiment a singlet at δ –415 was observed (compare aniline with δ –320¹⁶). In the ¹³C{¹H} NMR spectrum the signals of the phenyl carbon atoms appear as pseudotriplets, and therefore, the ¹³C,¹⁵N coupling constants are not deducible (Table 2). The only exception is the triplet for the ZnMe fragments,

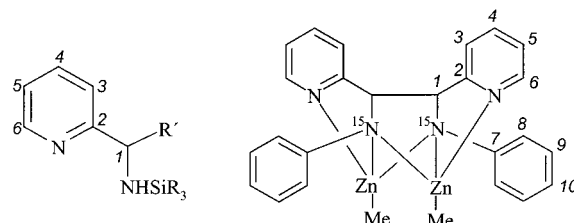


Figure 5. Numbering scheme for the assignments of the NMR parameters. On the left, the numbering scheme of the amines **3** and **4** is given, whereas on the right side, the scheme for the dinuclear zinc complex **5** is presented.

Table 1. Selected NMR Parameters of Compounds **2–4**^a

	3	3 ·H ₂ O	4
¹ H NMR			
δ(H1)	4.72	4.72	4.46
δ(H3)	7.36	7.37	6.81
δ(H4)	7.11	7.12	6.95
δ(H5)	6.64	6.40	6.56
δ(H6)	8.48	8.47	8.45
δ(SiMe)	–0.22	–0.22	–0.04
δ(SiMe)	–0.30	–0.31	–0.08
δ(tBu)	0.85	0.85	0.89
δ(NH)	2.41	2.40	2.30
¹³ C{ ¹ H} NMR			
δ(C1)	63.56	63.56	64.31
δ(C2)	164.87	164.87	164.94
δ(C3)	121.20	121.20	121.05
δ(C4)	135.36	135.36	134.86
δ(C5)	121.95	121.96	122.60
δ(C6)	148.29	148.29	148.79
δ(SiMe)	–4.93	–4.92	–4.67
δ(SiMe)	–5.48	–5.47	–4.91
δ(CMe ₃)	18.26	18.27	18.14
δ(CMe ₃)	26.29	26.30	26.32
²⁹ Si{ ¹ H} NMR			
δ(SiMe ₂ Bu)	8.48	9.37	9.28

^a Conditions: solvent [D₆]benzene, 30 °C.

Table 2. NMR Data of the ¹⁵N-Labeled Compound **5a**^a

	δ(¹ H)	δ(¹³ C{ ¹ H})	ⁿ J + ⁿ⁺² J(¹³ C, ¹⁵ N)
C1/H1	4.38	65.7	
C2		165.5	
C3/H3	7.88	122.9	
C4/H4	7.98	139.5	
C5/H5	7.37	123.5	
C6/H6	8.31	147.6	
C7		154.4	7.7 Hz (<i>n</i> = 1) ^b
C8/H8	6.73	117.0	3.5 Hz (<i>n</i> = 2) ^c
C9/H9	6.83	128.1	1.7 Hz (<i>n</i> = 3)
C10/H10	6.37	116.0	<0.7 Hz (<i>n</i> = 4)
Zn–CH ₃	–0.42	–17.9	<i>d</i>

^a Conditions: [D₈]THF, 30 °C. ^b ¹J(¹³C,¹⁵N) = –6.7 Hz, ³J(¹³C,¹⁵N) = –1.0 Hz. ^c ²J(¹³C,¹⁵N) = 3.8 Hz, ⁴J(¹³C,¹⁵N) = –0.3 Hz, ³J(¹⁵N,¹⁵N) = 8.2 Hz; see text. ^d Triplet, ²J(¹³C,¹⁵N) = 2.3 Hz.

with a ²J(¹³C,¹⁵N) value of 2.3 Hz. All other coupling patterns allow the determination of the sum of the coupling constants $N = {}^nJ({}^{13}\text{C}, {}^{15}\text{N}) + {}^{n+2}J({}^{13}\text{C}, {}^{15}\text{N})$. However, the contribution of the long-range couplings should be much smaller. From the ¹³C{¹H} resonance of the ortho phenyl carbon atom at δ 117.0, which shows all five signals of the X part of an AA'X pattern, a rather large ³J(¹⁵N,¹⁵N) value of 8.2 Hz was calculated (²J(¹³C,¹⁵N) = 3.8 Hz; ⁴J(¹³C,¹⁵N) = –0.3 Hz; ³J(¹⁵N,¹⁵N) = 8.2 Hz, see Figure 6 and also refs 17 and 18). The large coupling constant results from a cis arrangement

(16) Hesse, M.; Meier, H.; Zeeh, B. *Spektroskopische Methoden in der organischen Chemie*, 5th ed.; Stuttgart, Germany, 1995; p. 209.

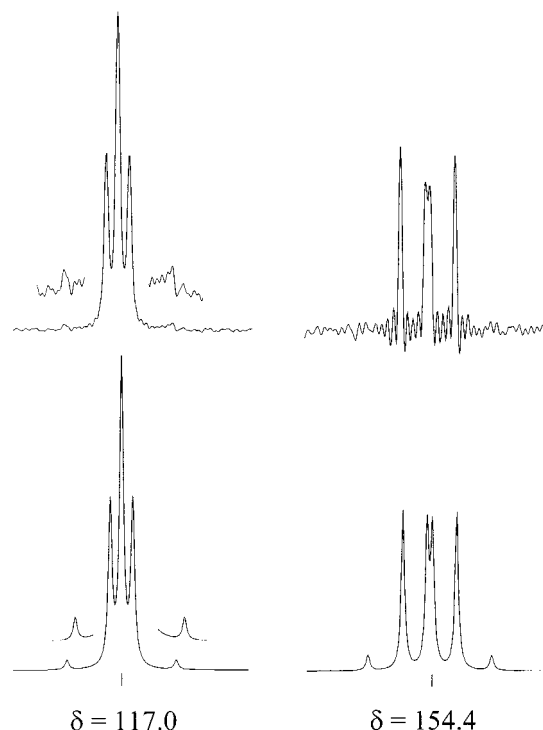


Figure 6. Coupling pattern of the observed (above) and calculated (below) $^{13}\text{C}\{^1\text{H}\}$ NMR signals of the ortho (left) and ipso phenyl carbon atoms (right) of **5a** (see text; solvent $[\text{D}_8]\text{THF}$, 30°C).

of the N atoms in the four-membered Zn_2N_2 ring as well as the 3-fold connection via the zinc atoms and the C_2 fragment. The positive sign of $^2J(^{13}\text{C},^{15}\text{N})$ was chosen, and consequently, the negative sign of $^4J(^{13}\text{C},^{15}\text{N})$ was enforced. For the ipso carbon atom of the phenyl substituent at δ 154.4, an additional isotropy effect of $^{12,13}\text{C}$ on ^{15}N was observed (Figure 6). The middle resonance shows a splitting which accounts for different chemical environments of the ^{15}N atoms and the AA'X system (five resonances for the X part) changes to an ABX spin system with six lines for the X part. The value of the isotropy effect amounts to 28.6 ppb and is larger than, for example, in nitromethane (19 ppb¹⁹). This value was calculated from the ^{13}C NMR signals of the ipso carbon atom with a coupling of $^3J(^{15}\text{N},^{15}\text{N}) = 8.2$ Hz under variation of the chemical shifts of N and the $^{13}\text{C},^{15}\text{N}$ coupling constants. From the intensity ratios of the outer signals to the inner resonances $^nJ(\text{C},\text{N})$ values are deducible ($^1J(^{13}\text{C},^{15}\text{N}) = -6.7$ Hz and $^3J(^{13}\text{C},^{15}\text{N}) = -1.0$ Hz); experience shows that $^1J(^{13}\text{C},^{15}\text{N})$ coupling constants are usually negative.²⁰

Experimental Section

General Procedures. All experiments and manipulations were carried out under an atmosphere of argon. Reactions were performed by using standard Schlenk techniques and dried, thoroughly deoxygenated solvents. Starting materials were prepared according to literature procedures cited in the

Introduction. NMR spectra were recorded on JEOL GSX270 and EX400 spectrometers. A Nicolet 520 FT-IR spectrophotometer was used to record the IR spectra; solid substances were measured in Nujol between KBr plates.

Synthesis of (1*S*,2*S*)- and (1*R*,2*R*)-1,2-Dipyridyl-1,2-bis((*tert*-butyldimethylsilyl)amino)ethane (3**).** To 0.80 g of bis(methylzinc) 1,2-dipyridyl-1,2-bis((*tert*-butyldimethylsilyl)amido)ethane (**1**; 1.33 mmol) in 10 mL of toluene was added 0.34 g (5.72 mmol) of acetamide. The reaction mixture was stirred for 10 h at 20°C . The residue was separated from the solution and extracted a second time with pentane. From the unified solutions the majority of the solvent was removed under vacuum. During storage at 5°C 0.55 g of colorless 1,2-dipyridyl-1,2-bis((*tert*-butyldimethylsilyl)amino)ethane (**3**) crystallized (1.24 mmol, 93%). Mp: 66°C . The NMR data are summarized in Table 1. IR (Nujol, cm^{-1}): 3377 s, 3362 s, 1616 sh, 1589 vs, 1568 s, 1471 vs, 1465 sh, 1436 vs, 1414 vs, 1399 vs, 1359 s, 1315 m, 1291 w, 1257 vs, 1209 w, 1197 m, 1147 s, 1139 vs, 1115 vs, 1089 vs, 1048 vs, 1022 s, 1008 s, 995 m, 939 m, 919 s, 908 vs, 884 s, 830 vs, 807 vs, 779 sh, 762 s, 746 vs, 729 sh, 677 m, 660 s, 637 s, 623 m, 601 s, 564 w, 534 vw, 494 sh, 478 w, 455 w, 417 sh, 402 m, 361 w, 326 w, 296 vw, 279 vw. EI-MS (m/z): 222 (44%), 221 ($\text{M}^+/\text{2}$, 100%), 164 (11%), 163 (221 - C_4H_{10} , 18%), 73 ($\text{SiMe}_2\text{Bu} - \text{C}_3\text{H}_6$, 35%). Anal. Calcd for $\text{C}_{24}\text{H}_{42}\text{N}_4\text{Si}_2$ (442.80): C, 65.10; H, 9.56; N, 12.66. Found: C, 64.46; H, 9.87; N, 12.38.

Synthesis of (1*S*,2*S*)- and (1*R*,2*R*)-1,2-Dipyridyl-1,2-bis((*tert*-butyldimethylsilyl)amino)ethane Hydrate (3**· H_2O).** (1*S*,2*S*)- and (1*R*,2*R*)-1,2-dipyridyl-1,2-di(*tert*-butyldimethylsilylamino)ethane (**3**) was recrystallized from a acetone/water mixture, yielding colorless needles of the H_2O adduct (1*S*,2*S*)- and (1*R*,2*R*)-1,2-dipyridyl-1,2-di(*tert*-butyldimethylsilylamino)ethane hydrate (**3**· H_2O). Mp: 90°C . NMR parameters are listed in Table 1. IR (Nujol, cm^{-1}): 3407 s, 3370 vs, 3319 vs, 3238 vs, 2359 vw, 2294 vw, 1737 w, 1689 vs, 1629 vw, 1594 vs, 1567 vs, 1545 m, 1472 vs, 1461 sh, 1436 vs, 1389 s, 1359 s, 1337 sh, 1327 m, 1276 sh, 1256 vs, 1245 vs, 1213 m, 1185 w, 1138 sh, 1130 vs, 1087 vs, 1049 s, 1003 vs, 992 sh, 937 s, 919 vs, 884 s, 828 vs, 821 vs, 807 vs, 792 vs, 777 vs, 763 vs, 750 vs, 735 m, 684 sh, 672 vs, 661 s, 627 s, 605 vs, 564 w, 501 vw, 478 m, 462 m, 403 m, 366 s, 335 vw, 320 vw, 293 w.

Synthesis of (1*S*,2*R*)-1,2-Dipyridyl-1,2-bis((*tert*-butyldimethylsilyl)amino)ethane (4**).** A solution of (1*S*,2*S*)- and (1*R*,2*R*)-1,2-dipyridyl-1,2-bis((*tert*-butyldimethylsilyl)amino)ethane (**3**) in pentane was irradiated by a mercury lamp for 4 h at 15°C , yielding a mixture of 38% of **3**, 41% of **4**, and 21% of (2-pyridylmethyl)(*tert*-butyldimethylsilyl)amine. After the volume of the solvent was reduced, colorless needles of 1,2-dipyridyl-1,2-di((*tert*-butyldimethylsilyl)amino)ethane (**4**) crystallized at 5°C . NMR data are presented in Table 1. This compound was obtained as a mixture with the racemate of **3**, and therefore, further analytical data were not recorded.

Synthesis of (1*S*,2*S*)-Bis(methylzinc) and (1*R*,2*R*)-Bis(methylzinc) 1,2-Bis(phenylamido)-1,2-dipyridylethane (5**).** Bis(methylzinc) 1,2-dipyridyl-1,2-bis((*tert*-butyldimethylsilyl)amido)ethane (**2**; 0.72 g, 1.20 mmol) was dissolved in 7 mL of toluene, and 0.22 mL of aniline (2.4 mmol) was added at room temperature. Then the solution was heated under reflux for 2 h. During this time a precipitate formed, which was washed after filtration and then dissolved in THF. At 5°C colorless needles of bis(methylzinc) 1,2-dipyridyl-1,2-bis(phenylamido)ethane (**5**; 0.56 g, 1.06 mmol, 88%) crystallized. Mp: 106°C . NMR data of the ^{15}N -labeled derivative **5a** are listed in Table 2. IR (cm^{-1}): 1603 vs, 1591 vs, 1568 s, 1484 vs, 1441 s, 1385 vw, 1359 vw, 1329 w, 1297 s, 1281 m, 1257 vs, 1181 w, 1159 w, 1109 vw, 1081 w, 1043 w, 1026 w, 992 m, 965 vw, 953 vw, 911 m, 896 w, 872 w, 846 w, 782 m, 772 vw, 758s, 735 sh, 694 s, 666 m, 648 w, 617 sh, 568 vw, 535 w, 529 sh, 508 vw, 489 vw, 470 vw, 409 w, 399 w. Anal. Calcd for **5**, $\text{C}_{26}\text{H}_{26}\text{N}_4\text{Zn}_2$ (525.268): C, 59.45; H, 4.99; N, 10.67. Found: C, 59.29; H, 4.85; N, 10.19.

(17) Witanowski, M.; Webb, G. A. *Annu. Rep. NMR Spectrosc.* **1981**, *11B*, 1.

(18) Witanowski, M.; Webb, G. A. *Annu. Rep. NMR Spectrosc.* **1986**, *18*, 1.

(19) Strelenko, Yu. A.; Torocheshnikov, V. N.; Sergeyev, N. M. *J. Magn. Reson.* **1990**, *89*, 123.

(20) Witanowski, M.; Stefaniak, L.; Webb, G. A. *Annu. Rep. NMR Spectrosc.* **1993**, *25*, 1.

Table 3. Summary of Crystallographic Data of 3, 3·H₂O, and 4 as Well as Details of the Structure Solution and Refinement Procedures

	3	3·H₂O	4
empirical formula	C ₂₄ H ₄₂ N ₄ Si ₂	C ₂₄ H ₄₄ N ₄ O ₂ Si ₂	C ₂₄ H ₄₂ N ₄ Si ₂
fw	442.80	460.81	442.81
temp <i>T</i> (K)	193(2)	200(2)	193(2)
space group ²²	<i>C2/c</i> (No. 15)	<i>C2/c</i> (No. 15)	<i>P1</i> (No. 2)
unit cell dimens			
<i>a</i> (Å)	29.633(8)	26.2662(6)	6.2942(6)
<i>b</i> (Å)	11.465(3)	7.0838(2)	10.568(1)
<i>c</i> (Å)	15.962(4)	18.4572(6)	11.057(1)
α (deg)	90	90	80.812(1)
β (deg)	95.288(4)	123.368(1)	74.740(2)
γ (deg)	90	90	76.682(2)
<i>V</i> (Å ³)	5400(2)	2868.1(1)	686.6(1)
<i>Z</i>	8	4	1
ρ _{calcd} (g cm ⁻³)	1.094	1.067	1.071
λ (Å)	0.710 73	0.710 73	0.710 73
μ (cm ⁻¹)	0.148	0.144	0.146
abs cor	SADABS	numerical	SADABS
<i>T</i> _{min} / <i>T</i> _{max}	0.555/0.856	0.968/0.995	0.811/1.000
no. of measd data	14 994	13 263	3999
no. of indep data	5083	1292	2103
no. of params	289	159	220
wR2 ^a (all data, on <i>F</i> ²)	0.1220	0.1668	0.1088
R1 ^a (all data)	0.0533	0.0841	0.0530
no. of data with <i>I</i> > 2σ(<i>I</i>)	4153	1110	1540
R1 ^a (<i>I</i> > 2σ(<i>I</i>))	0.0421	0.0608	0.0390
goodness of fit <i>s</i> ^b on <i>F</i> ²	1.020	1.309	0.959
residual density (e Å ⁻³)	0.407/−0.214	0.600/−0.651	0.156/−0.204

^a Definition of the *R* indices: $R1 = (\sum ||F_o| - |F_c||) / \sum |F_o|$; $wR2 = \{ \sum [w(F_o^2 - F_c^2)^2] / \sum [w(F_o^2)^2] \}^{1/2}$ with $w^{-1} = \sigma^2(F_o^2) + (aP)^2$.²⁶ ^b $s = \{ \sum [w(F_o^2 - F_c^2)^2] / (N_o - N_p) \}^{1/2}$.

Synthesis of 1,2-Bis(phenylamido)-1,2-dipyridylethane (6). Bis(methylzinc) 1,2-dipyridyl-1,2-bis(phenylamido)ethane (**5**; 0.30 g, 0.57 mmol) was dissolved in 15 mL of toluene, and 0.14 g of acetamide (2.39 mmol) was added at 0 °C. The solution was stirred for 12 h at room temperature. The colorless precipitate was collected and washed with toluene. At −18 °C 0.10 g of 1,2-bis(phenylamido)-1,2-dipyridylethane (**6**; 0.27 mmol, 48%) crystallized in the shape of extremely thin and colorless needles. Mp: 182 °C. ¹H NMR ([D₈]toluene, numbering scheme according to Figure 5): δ 8.34 (H6), 6.98 (H9), 6.87 (H3), 6.78 (H4), 6.60 (H10), 6.51 (H5), 6.50 (H8), 6.05 (NH, ¹J(¹⁵N,H) = 86.2 Hz), 5.14 (H1, multiplet). ¹³C{¹H} NMR ([D₈]toluene): δ 148.4 (C6), 135.8 (C4), 129.1 (C9), 122.0 (C3), 121.8 (C5), 117.6 (C10), 113.6 (C8), 67.4 (C1), quaternary C2 and C7 were not observed due to solubility problems in

toluene. ¹⁵N{¹H} NMR ([D₈]toluene): δ −314.3 (NH). IR (cm⁻¹): 3375 m, 3310 m, 1671 vw, 1602 vs, 1591 vs, 1569 m, 1500 vs, 1473 s, 1438 vs, 1428 vs, 1382 s, 1348 m, 1340 sh, 1314 vs, 1293 sh, 1277 s, 1265 s, 1248 w, 1211 vw, 1181 m, 1155 m, 1147 sh, 1125 m, 1098 m, 1087 w, 1081 sh, 1068 w, 1048 m, 1029 w, 994 m, 966 w, 898 vw, 885 vw, 869 m, 840 vw, 829 vw, 813 vw, 787 s, 768 w, 754 s, 746 vs, 723 m, 698 m, 689 s, 675 w, 662 vw, 619 w, 595 vw, 555 vw, 531 vw, 510 sh, 502 m, 465 vw, 430 vw. EI-MS (*m/z*): 368 (4%, M⁺), 185 (100%), 184 (97%, M^{+/2}), 107 (13%), 77 (10%).

Crystal Structure Determinations. Data were collected on a Siemens P4 diffractometer with a Siemens SMART-CCD area detector (**3** and **4**) and on a Stoe-IPDS diffractometer (**3·H₂O**) with graphite-monochromated Mo Kα radiation (λ = 0.710 73 Å) using oil-coated rapidly cooled single crystals.²¹ Absorption corrections were applied as given in Table 3. Crystallographic parameters, details of data collection and refinement procedures are also summarized in Table 3.

The structures were solved by direct methods and refined with the software packages SHELXL-93 and SHELXL-97.²³ Neutral scattering factors were taken from Cromer and Mann²⁴ and, for the hydrogen atoms, from Stewart et al.²⁵ The non-hydrogen atoms were refined anisotropically. The H atoms were considered with a riding model under restriction of ideal symmetry at the corresponding carbon atoms. The H atoms of the methyl substituents were considered with the riding model, whereas for **4** all hydrogen atoms were refined isotropically.

Acknowledgment. We thank the Fonds der Chemischen Industrie (Frankfurt/Main, Germany) and the Deutsche Forschungsgemeinschaft (Bonn, Germany) for generous financial support. T.B. wishes to express his gratitude to the Fonds der Chemischen Industrie for a Ph.D. scholarship granted.

Supporting Information Available: Listings of crystal data, atomic coordinates, bond lengths and angles, and anisotropic displacement parameters of non-hydrogen atoms for **3**, **3·H₂O**, and **4**. This material is available free of charge via the Internet at <http://pubs.acs.org>.

OM010867L

(21) Kottke, T.; Stalke, D. *J. Appl. Crystallogr.* **1993**, *26*, 615. Stalke, D. *Chem. Soc. Rev.* **1998**, *27*, 171.

(22) Hahn, T., Ed. *International Tables for Crystallography*, 2nd ed.; D. Reidel: Dordrecht, The Netherlands, 1984; Vol. A (Space Group Symmetry).

(23) Sheldrick, G. M. SHELXL-93; Universität Göttingen, 1993. SHELXL-97; Universität Göttingen, 1997.

(24) Cromer, D. T.; Mann, J. B. *Acta Crystallogr.* **1968**, *24*, 321.

(25) Stewart, R. F.; Davidson, E. R.; Simpson, W. T. *J. Chem. Phys.* **1965**, *42*, 3175.